



Properties of amorphous SiAlON thin films grown by RF magnetron co-sputtering



G.P. Bernhardt, J.I. Krassikoff¹, B.T. Sturtevant², R.J. Lad^{*}

Laboratory for Surface Science & Technology, University of Maine, Orono, ME 04469-5708, USA

ARTICLE INFO

Article history:

Received 26 January 2014

Accepted in revised form 3 July 2014

Available online 10 July 2014

Keywords:

SiAlON films

RF magnetron co-sputtering

Amorphous structure

High temperature oxidation

Wear resistance

ABSTRACT

SiAlON thin films were deposited by RF magnetron co-sputtering of Al and Si targets in Ar/O₂/N₂ mixtures to a thickness of ~200 nm onto both bare and Pt-coated r-cut sapphire substrates. Films deposited at 200 °C are amorphous as determined from X-ray diffraction (XRD) and have <1 nm RMS roughness as measured by X-ray reflectivity (XRR). *In situ* X-ray photoelectron spectroscopy (XPS) measurements from films grown over a wide range of Si_xAl_yO_zN_{100-x-y-z} stoichiometries indicate that a homogenous amorphous phase is formed over all compositional regions of the quaternary thin film phase diagram. After annealing at 1000 °C for 10 h in vacuum, the film stoichiometries remained nearly unchanged and the films retained an amorphous structure, as verified by XRD. The films lost nitrogen during air exposure at 1000 °C, leading to the formation of an amorphous aluminum silicate layer at the surface. No crystalline SiAlON phases, which have been reported for bulk SiAlON materials, were observed in films even after heating at 1500 °C for 10 days. Pin-on-disk measurements showed that SiAlON films have negligible wear up to 80 gram loads, while significant wear occurs on the sapphire pin in sliding contact, indicating that the SiAlON films have excellent wear resistance.

© 2014 Elsevier B.V. All rights reserved.

1. Introduction

Sintered SiAlON bulk ceramics have received considerable attention since their initial development during the 1970s [1–5]. These materials, which can exist over a range of Si_xAl_yO_zN_{100-x-y-z} stoichiometries, contain a network of Si(O,N)₄ and Al(O,N)₄ structural groups with short-range order, and can be viewed as aluminum silicates in which some of the oxygen anions are replaced by nitrogen anions. Combining oxide and nitride properties into SiAlON alloys yields excellent hardness, wear, and fracture toughness, making SiAlON materials useful in applications such as cutting tools and high temperature structural components [6,7]. Fig. 1 shows a quaternary composition diagram for the 4-component Si–Al–O–N system [1]. Each Si_xAl_yO_zN_{100-x-y-z} stoichiometry can be represented as a point on this diagram using the charge neutrality condition $4x + 3y - 2z - 2(1 - x - y - z) = 0$ along with the relationship between atomic concentrations and atomic percentages; i.e. $[Al] / ([Al] + [Si]) = x / (x + y)$ and $[O] / ([O] + [N]) = z / (100 - x - y)$. The composition diagram indicates several of the well known bulk phases, including the β' phase that is isostructural with β-Si₃N₄, the X phase that is isostructural with mullite, the O' phase that is isostructural with Si₂N₂O, and several AlN-like polytype

phases. In bulk form, SiAlON materials have been produced primarily by reaction sintering or combustion synthesis [8–10]. The β'-SiAlON composition, which has a stoichiometry of Si_{6-z}Al₂O₂N_{8-z}, has been emphasized in most bulk studies because it has extreme toughness [9, 10], but recent investigations have shown that adding interstitial dopants to form an α-SiAlON material leads to a chemically more complex but potentially harder material [4,5,11].

While synthesis methods of bulk SiAlON materials are well developed, relatively little work has been done in the area of SiAlON thin film synthesis. Bodart et al. [12–14] used ion implantation of oxygen and nitrogen into sputtered Si_xAl_y coatings to create homogeneous SiAlON coatings layers. Unbalanced DC and RF sputter deposition of SiAlON thin films have also been reported [15,16], but minimal characterization was performed on these films. A recent report also shows that hard SiAlON films, grown by ion beam deposition on optically transparent zinc sulfide windows, perform well in harsh environmental conditions [17]. In our work, we have precisely controlled the RF magnetron co-sputtering film deposition process to deposit a range of homogeneous Si_xAl_yO_zN_{100-x-y-z} films with nominal thickness of 200 nm, and we report the results of experiments that probed their stoichiometry, structure, bonding, oxidation, and wear.

2. Materials and methods

Several different RF magnetron sputtering targets were tried in Ar/N₂/O₂ gas mixtures for depositing the SiAlON films, including alloy (SiAlON, AlN, SiO₂) and elemental (Si, Al) targets. Films grown using a

* Corresponding author.

E-mail address: rjad@maine.edu (R.J. Lad).

¹ Current address: Raytheon Missile Systems, Tucson, AZ 85706, USA.

² Current address: Los Alamos National Laboratory, Los Alamos, NM 87545, USA.

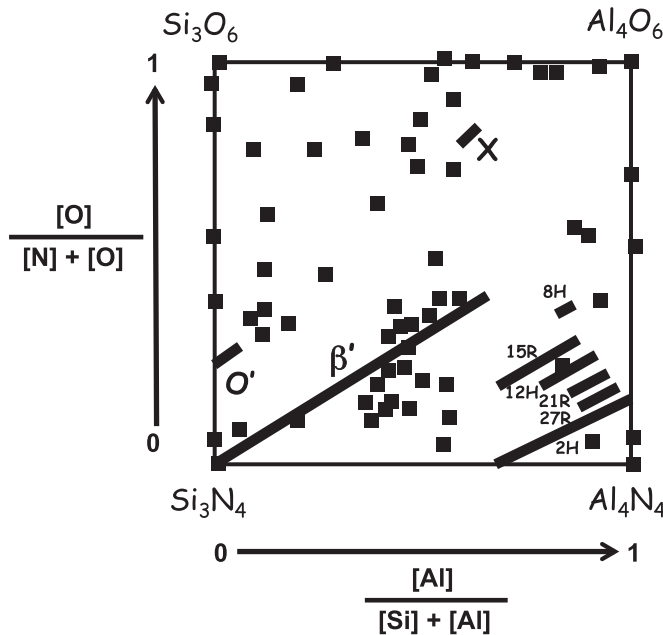


Fig. 1. SiAlON film compositions synthesized in this study as determined by XPS analysis (squares) plotted on the bulk quaternary composition diagram for the 4-component Si–Al–O–N system. After Ref [1].

sintered SiAlON sputter target had significant iron contamination (~2 at.%), and films deposited from AlN and SiO₂ targets led to poorly controlled film compositions with very low nitrogen content. Co-sputtering of elemental Si and Al targets in 50% Ar + 50% N₂/O₂ gas mixtures yielded the necessary control to achieve reproducible depositions for films over a wide range of stoichiometries.

The SiAlON films were grown at 200 °C onto either uncoated or Pt-coated *r*-cut (01 $\bar{1}2$) oriented sapphire (α -Al₂O₃) substrates that were 15 mm × 15 mm in size within a film deposition system with base pressure <1 × 10⁻⁹ Torr [18]. Films were grown to thicknesses ranging from 10 nm to 2 μ m, but unless otherwise noted, the results shown in this paper are for films with 200 nm nominal thicknesses. The Pt-coated sapphire substrates, consisting of a 50 nm Pt layer over a 10 nm Zr adhesion layer [19], were used in order to minimize charging effects during X-ray photoelectron spectroscopy (XPS) measurements. Prior to SiAlON film deposition, the substrates were cleaned with acetone, isopropyl alcohol, and DI water, and then inserted into vacuum and exposed to an Ar⁺ plasma generated by a 150 W, electron cyclotron resonance (ECR) source operating at 10⁻⁴ Torr. This procedure removed any hydrocarbon contamination and yielded atomically clean sapphire surfaces as verified by XPS and reflection high energy electron diffraction (RHEED).

The parameters that were controlled during each SiAlON film deposition included the N₂/O₂ gas flow rate, total gas pressure, RF magnetron power, and substrate temperature. Deposition rates were measured during the growth of SiO₂, AlN, Al₂O₃, and Si₃N₄ films using a quartz crystal oscillator (QCO), and these rates were used to determine the conditions needed to get SiAlON films with the desired stoichiometry and thickness. SiAlON films spanning the full Si:Al and O:N composition ranges were synthesized by adjusting the RF power applied to each sputter target to control the relative Si and Al fluxes and regulating the gas composition of the 50% N₂/O₂ + 50% Ar plasma at a total pressure of 3 mTorr. Since the relative difference in sticking/reactivity of oxygen versus nitrogen plasma species is very large, it was found that N₂/O₂ ratios between 94:6 and 99:1 were appropriate to yield SiAlON compositions over the entire O:N range.

Immediately following deposition, the films were transferred under ultra-high vacuum to an XPS analysis chamber to measure the film stoichiometry. RHEED was also conducted *in situ* using a 30 keV electron gun. Once brought into the air, the films were characterized by X-ray diffraction (XRD), X-ray reflectivity (XRR), surface profilometry, and pin-on-disk wear tests. Some films were also heated in air between 1000 °C–1500 °C in a tube furnace and subsequently analyzed by XPS and XRD.

3. Results

3.1. Film stoichiometry and structure

The stoichiometries of the SiAlON films investigated in this study (symbols in Fig. 1) were determined by *in situ* XPS using normal and glancing take-off angles. Fig. 2 shows an XPS spectrum from a representative SiAlON film acquired using Mg K α X-rays. Both the core level and KLL Auger peaks for O, N, Si, and Al are plotted as relative binding energy; the Si and Al Auger peaks were excited by the bremsstrahlung radiation from the X-ray source. The stoichiometry of each film was determined from the relative XPS peak areas corrected by a Shirley background and using CasaXPS Element Library sensitivity factors. To estimate the measured error in stoichiometry, five films were grown using identical deposition parameters and then analyzed by XPS. Film stoichiometries were found to be within $\pm 3\%$ for both the Si/(Si + Al) and N/(N + O) ratios. Also, XPS measurements of as-deposited films during Ar⁺ ion depth profiling (not shown) at several locations across the films revealed that the film compositions were both laterally homogeneous as well as homogenous throughout the thickness of the films.

XRD spectra acquired from all films deposited at 200 °C exhibited a diffuse ~15° wide peak centered near $2\theta = 13^\circ$ indicating that the films were amorphous. RHEED patterns immediately after deposition also showed only an amorphous diffuse background. XRR analysis was performed to measure the film density, thickness, and roughness, as shown by the example in Fig. 3 for a Si₁₉Al₂₀O₂₀N₄₁ film. Using PANalytical X'Pert Reflectivity software, simulated XRR spectra were created assuming a single uniform layer on a thick substrate, and compared to the measured XRR data. The analysis for the spectrum in Fig. 3 yielded a film density of 2.8 g/cm³ as determined from the critical angle, $\theta_c = 0.24^\circ$, and a film thickness of 21 nm and growth rate of 0.055 nm/s as calculated from the spacing, $\Delta\theta = 0.078^\circ$, of the Kiessig interference fringes [20]. Based on modeling of the very small attenuation level of the Kiessig fringes, the film roughness was determined to be <1 nm over the several mm² area probed by the X-ray beam. Except for different Kiessig fringe

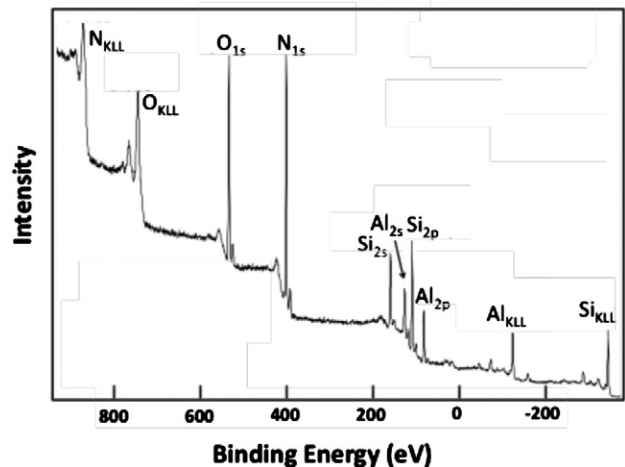


Fig. 2. XPS spectrum from an as-grown film with composition Si₂₅Al₂₄O₁₇N₃₄ showing core level and KLL Auger peaks.

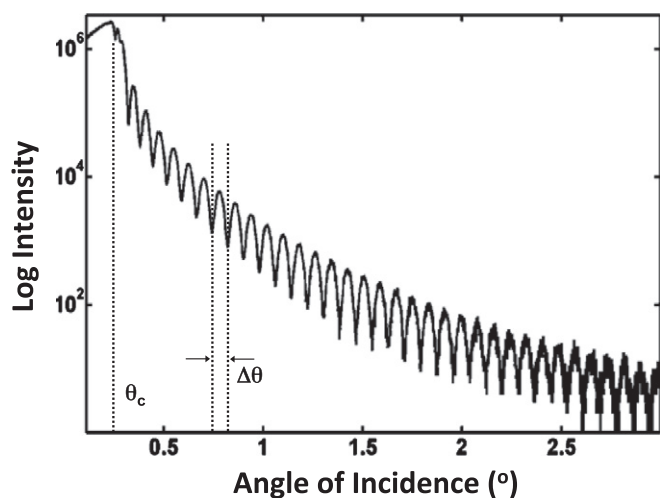


Fig. 3. XRR spectrum from $\text{Si}_{1.9}\text{Al}_{2.0}\text{O}_{2.0}\text{N}_{4.1}$ film showing critical angle $\theta_c = 0.24^\circ$ and multiple Kiessig interference fringes with spacing $\Delta\theta = 0.078^\circ$.

spacings that depended on specific thickness, XRR spectra from films covering the full range of O:N and Al:Si ratios were essentially the same, indicative of a very smooth amorphous film structure.

3.2. Chemical bonding

In situ high resolution XPS measurements of the Auger and core levels were acquired from films grown over a wide range of $\text{Si}_x\text{Al}_y\text{O}_z\text{N}_{100-x-y-z}$ stoichiometries. Fig. 4 shows the O_{KLL} and N_{KLL} Auger spectra and Si 2s,2p + Al 2s,2p core levels for films with nearly equal Al:Si ratio and varying O:N ratio. Likewise, Fig. 5 shows Al_{KLL} and Si_{KLL} and N1s and O1s spectra from films with an approximately equal O:N ratio and varying Al:Si ratio. Each XPS spectrum was corrected for steady state charging (~ 6 eV) by aligning O1s to 530.1 eV, the same value as for an atomically clean r-cut sapphire surface [21]. This correction procedure allows accurate relative binding energy shifts of all the spectral peaks to be determined between samples.

As the Si:Al ratio in SiAlON films is varied (Fig. 4), the Si 2s, 2p and Al 2s, 2p core level emission shows the expected positions for Si^{4+} and Al^{3+} valence states and plasmon loss features at ~ 20 eV higher binding energy. In addition, the spectra lineshapes are similar for all SiAlON compositions, and no major binding energy shifts are observed, which suggests that the SiAlON films are homogenous and form a complete solid solution over the quaternary compositional ranges. The O_{KLL} and N_{KLL} lineshapes also do not change, including the Auger fine structure. For films over a range of O:N stoichiometries, the Al modified Auger parameter, $\alpha'_{\text{Al}} = \text{KE}(\text{Al}_{\text{KLL}}) - \text{BE}(\text{Al}2\text{p})$, which depends on the extra-atomic relaxation energies [22], was found to be within a band of values, 1461.9 ± 0.9 eV, and the Si modified Auger parameter, $\alpha'_{\text{Si}} = \text{KE}(\text{Si}_{\text{KLL}}) - \text{BE}(\text{Si}2\text{p})$, was 1713.8 ± 0.5 eV, where KE and BE refer to kinetic energy and binding energy, respectively. In general, α'_{Al} and α'_{Si} increased slightly as the amount of nitrogen in the film increased, indicative of the bonding being more covalent. The Auger parameter values for the SiAlON films are also consistent with those reported for other aluminum–oxygen and silicon–oxygen–nitrogen compounds [22,23]. The observation of only small variations in the Auger parameters as the O:N film composition is changed over a large range indicates that the electronic interactions with the surrounding atoms do not vary significantly as a function of stoichiometry.

As the O:N ratio in SiAlON films is varied (Fig. 5), the Si_{KLL} and Al_{KLL} peak shapes remain unchanged, again consistent with homogenous amorphous films. The O1s, charge referenced to 530.1 eV, remains a

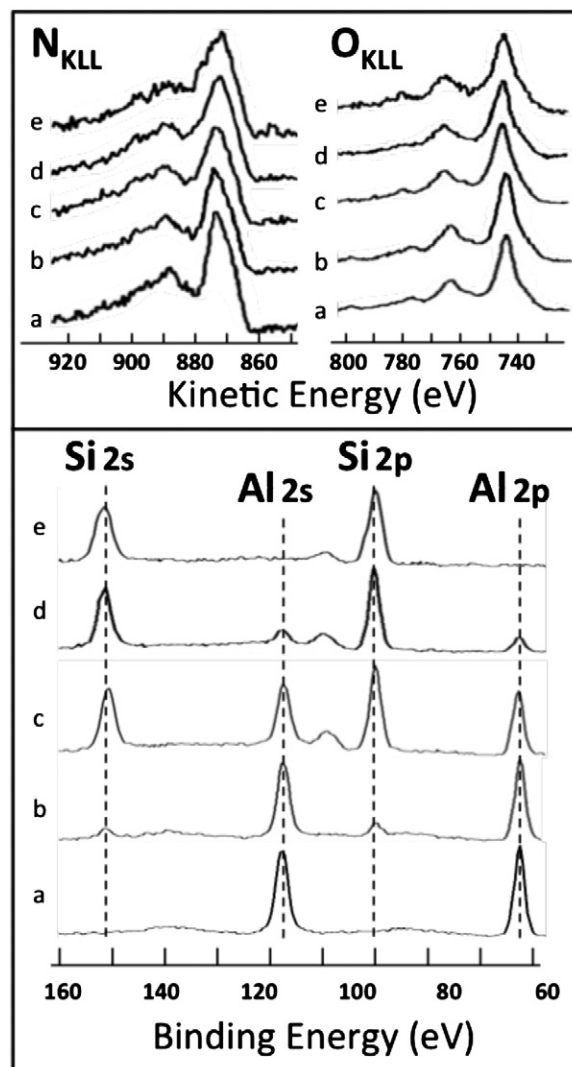


Fig. 4. N_{KLL} and O_{KLL} Auger spectra and Si 2s,2p + Al 2s,2p core levels for SiAlON films with nearly equal O:N ratio and varying Si:Al ratio. The Si/(S + Al) ratio is (a) 0.05, (b) 0.12, (c) 0.38, (d) 0.76, and (e) 0.97.

symmetric single peak, and the N1s binding energy of 397.5 eV is characteristic of Si–N or Al–N bonds. For films with oxygen content $(\text{O}/\text{O} + \text{N}) > 0.8$, a second N1s peak emerges at ~ 5 eV higher binding energy, which has also been observed in XPS studies of silicon oxynitride films [24]. This high binding energy N1s feature is influenced primarily by nearest neighbor electronegative atoms. As the oxygen concentration gets large enough, many of the nitrogen atoms begin to have more oxygen nearest neighbors and these N–O bonds exhibit a large N1s shift to higher binding energy. The main N1s line is still prevalent from nitrogen atoms also being coordinated to neighboring Al and Si atoms.

3.3. Wear behavior

Pin-on-disk measurements at room temperature were conducted on SiAlON films to measure film wear. Each film was subjected to sliding wear testing in contact with a polished spherical sapphire pin using normal loads from 1 to 80 g, with a contact radius of ~ 40 μm . The sliding speed was kept constant at 0.6 m/min and the wear track radius was varied from 1.5 mm to 7 mm with a total sliding distance of 10 m. Following each test, the pin surface was examined with optical

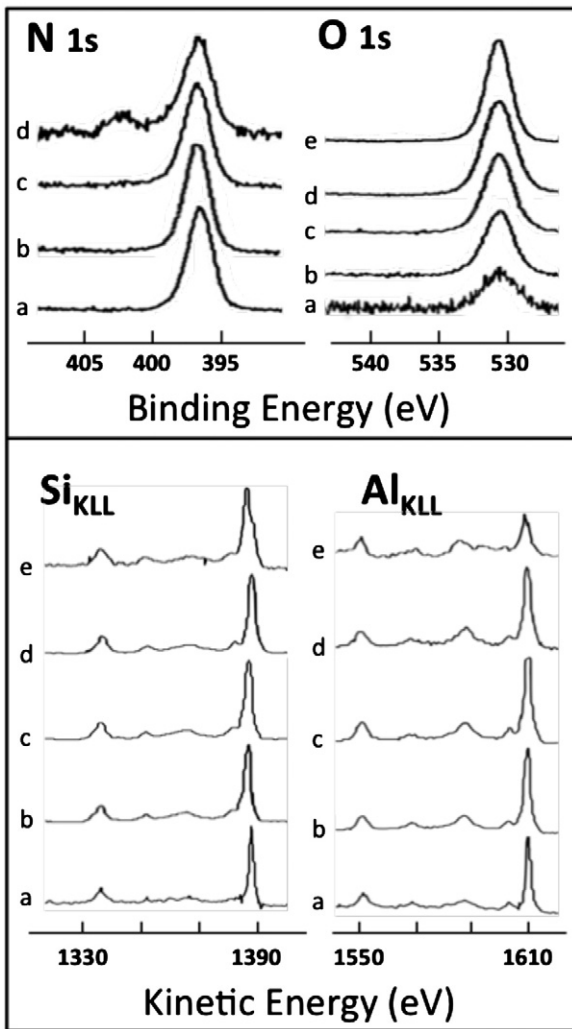


Fig. 5. Al_{KLL} and Si_{KLL} Auger and N_{1s} and O_{1s} core level spectra from SiAlON films with nearly equal Al:Si ratio and varying O:N ratio. The O/(O + N) ratio is (a) 0.07, (b) 0.33, (c) 0.52, (d) 0.80, and (e) 1.0.

microscopy and the wear track was analyzed using surface profilometry. Fig. 6 shows the wear tracks for two different N:O film compositions with approximately equal amounts of Al and Si. For the nitrogen-rich film, an optical microscopy image shows wear of the sapphire pin, but little wear of the SiAlON film until the load was increased to >40 g. Oxygen-rich SiAlON films appeared to be harder, leading to more wear of the sapphire pin and debris on the film surface at lower loads. Evidence for scratches and wear of the SiAlON film was not visible until the load was increased to 80 g. Pin-on-disk measurements taken on several other oxygen-rich and nitrogen-rich SiAlON films showed qualitatively similar results. Quantitative wear experiments are beyond the scope of this paper.

3.4. Film oxidation at high temperature

SiAlON films with different compositions were subjected to post-deposition annealing in lab air at temperatures between 1000 °C–1500 °C in an alumina crucible placed in a tube furnace that was ramped to temperature at 10 °C/min and held for several time intervals up to 10 days. Following air annealing at 1000 °C for >2 h, XPS showed that the nitrogen level in each of the films was reduced to zero within the XPS sampling depth (~10 nm). An XPS depth profile using Ar^+ etching showed nitrogen present below the surface, and the

depth of the nitrogen depletion layer was dependent on annealing time at 1000 °C, indicating that an aluminum silicate compound is formed at the film surface by oxidation from the gas phase. X-ray diffraction failed to show any evidence of crystalline structure even after air annealing treatments as high as 1500 °C for as long as 240 h. SiAlON films annealed in vacuum at 1000 °C for 10 h retained their nitrogen content and had a negligible change in film composition, and they retained an amorphous structure as verified by XRD.

4. Discussion

During RF magnetron sputtering, the O_2 and N_2 pressures were large enough for the cations in the SiAlON films to reach their maximum valence states (Al^{3+} and Si^{4+}). In such a case, the $Si_xAl_yO_zN_{100-x-y-z}$ film stoichiometries are subject to the charge neutrality condition: $4x + 3y - 2z - 3(100 - x - y - z) = 0$. The XPS and XRD results show that as-deposited SiAlON films are amorphous and have a homogenous composition. The fact that there are only small changes in the Al and Si Auger parameters as film stoichiometry is varied suggests that the local polarizability of Al–O and Si–O bonds are similar. The SiAlON structural building block is composed of 3-dimensional linkages of $(Si,Al)(O,N)_4$ tetrahedra. The character of the chemical bonding would be expected to change from covalent to ionic as the $(Si^{4+} + N^{3-})/(Al^{3+} + O^{2-})$ ratio decreases. However, a comparison of the measured α'_{Al} and α'_{Si} parameters with database values [23] suggests that the SiAlON films have a significant covalent character.

Our XPS results also agree with theoretical calculations of chemical bonding and atomic ordering effects in β -SiAlON by Okatov and Ivanovskii [25]. They performed tight-binding band calculations using large atomic cells based on the β - Si_3N_4 lattice and considered energetics as a function of replacing some Al for Si and some O for N atoms in the structure. Adding Al atoms into the Si_3N_4 lattice depopulates bonding states near the Fermi level and destabilizes the system. Likewise, O atom substitution causes antibonding states to become filled by the excess oxygen electrons, which also increases the system energy. However, if pairs of Al–O atoms are introduced, the bonding states are completely occupied and the antibonding states remain vacant. Hence, the total band energy is minimized when short-range atomic ordering occurs, with preference for Al–O bonds locally forming at the expense of Al–N and Si–O bonds. Density functional theory calculations for β -SiAlON by Fang and Metselaar [26] also conclude that Al–O and Si–N bonds are energetically more stable than Si–O and Al–N bonds. A driving force for preferred Al–O and Si–N bond creation as Al or Si

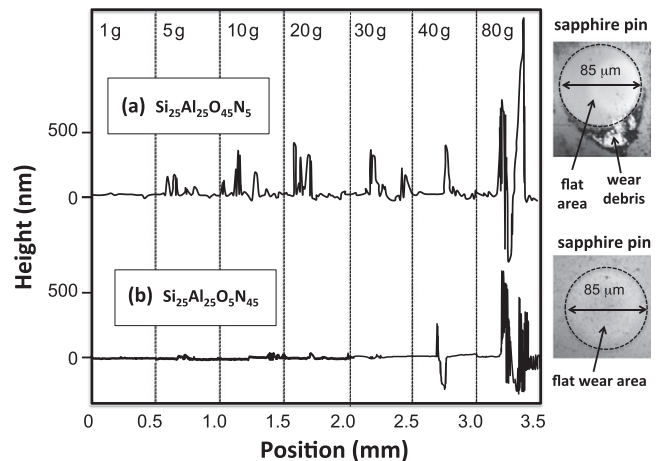


Fig. 6. Surface profilometry traces across the wear track as a function of load after a pin-on-disk test from an oxygen-rich and nitrogen-rich SiAlON film. The optical microscope image of wear on the sapphire pin shows a flat worn area on the sapphire pin for each case.

species from the sputter plasma arrive at the growing film surface may explain the solid solubility as the SiAlON composition is varied, as observed in our XPS measurements.

The high wear of the sapphire pin (Mohs hardness = 9 [27]) and minimal wear of the SiAlON films during sliding contact in a pin-on-disk test indicates that the SiAlON films have an excellent wear resistance. The homogeneous glassy structure and smooth surface morphology of SiAlON films, coupled with their wear resistance, suggests that they may be useful as a protective layer on a variety of sensors and MEMS devices. This is borne out in recent reports of SiAlON films being used as beneficial protective layers on infrared photodetectors [17] and microwave acoustic sensor devices [28].

5. Conclusions

SiAlON thin films deposited by RF magnetron co-sputtering of Al and Si targets in Ar/O₂/N₂ mixtures are promising smooth glassy coating materials for applications both at room temperature and at temperatures > 1000 °C. An amorphous structure and smooth surface morphology is present for all Si_xAl_yO_zN_{100-x-y-z} film compositions, and films deposited at 200 °C are homogeneous with no evidence of segregation or precipitated phases. Pin-on-disk measurements indicate that SiAlON films are harder than sapphire and have negligible wear up to 80 gram loads, indicating that SiAlON films have excellent wear resistance. Annealing SiAlON films above 1000 °C in air causes nitrogen depletion and aluminum silicate formation in the surface region of the films.

Conflict of interest

There is no conflict of interest for the work described in this paper.

Acknowledgments

The authors are grateful to D. Frankel and M. Call for many helpful suggestions. This work was supported by the National Science Foundation under Grant # DMR-0840045.

References

- [1] K.H. Jack, *J. Mater. Sci.* 11 (1976) 1135–1158.
- [2] A. Rosenflanz, *Curr. Opin. Solid State Mater. Sci.* 4 (1999) 453–459.
- [3] W. Schnick, *Int. J. Inorg. Mater.* 3 (2001) 1267–1272.
- [4] K. Komeya, M. Mitomo, Y.B. Cheng (Eds.), *Proc. of the Inter. Symp. on SiAlONs*, Trans Tech Publications LTD, Switzerland, 2003.
- [5] S. Hampshire, *J. Non-Cryst. Solids* 316 (2003) 64–73.
- [6] X. Tian, J. Zhao, J. Zhao, Z. Gong, Y. Dong, *Int. J. Adv. Manuf. Technol.* 69 (2013) 2669–2678.
- [7] X.C. Li, M.H. Fang, S.S. Chen, Y.G. Liu, Z.H. Huang, *Rare Metal Mater. Eng.* 42 (2013) 915–917.
- [8] G. Lui, K. Chen, J. Li, *Mater. Manuf. Process.* 28 (2013) 113–125.
- [9] X. Yi, J. Niu, T. Nakamura, T. Akiyama, *J. Alloys Compd.* 561 (2013) 1–4.
- [10] M. Shahien, M. Radwan, S. Kirihara, Y. Miyamoto, T. Sakurai, *J. Eur. Ceram. Soc.* 30 (2010) 1925–1930.
- [11] G.Z. Cao, R. Metselar, *Chem. Mater.* 3 (1991) 242–253.
- [12] M. Jacobs, F. Bodart, G. Terwagnea, D. Schryversb, A. Pouletc, *Nucl. Instrum. Phys. Res. B* 147 (1999) 231–237.
- [13] M. Jacobs, R. Bodart, *Surf. Coat. Technol.* 103–104 (1998) 113–117.
- [14] F. Bodart, M. Jacobs, *Nucl. Instrum. Phys. Res. B* 118 (1996) 714–717.
- [15] M. Jacobs, G. Terwagne, Ph. Rodquiny, F. Bodart, *Surf. Coat. Technol.* 116–119 (1999) 735–741.
- [16] O. Soichi, Y. Suzuki, M. Yoshitake, K. Natsukawa, in: J. Matsuo, G. Takaoka, I. Yamada (Eds.), *IEEE Proc. Ion Implantation Technol.*, 1998, pp. 775–778.
- [17] G. Liu, Z. Zhou, F. Fei, Q. Wei, H. Yang, Q. Liu, *Infrared Phys. Technol.* 60 (2013) 118–120.
- [18] S.C. Moulzolf, D.J. Frankel, R.J. Lad, *Rev. Sci. Instrum.* 73 (2002) 2325–2330.
- [19] G. Bernhardt, S. Silvestre, N. LeCursi, S.C. Moulzolf, D.J. Frankel, R.J. Lad, *Sensors Actuators B* 77 (2001) 368–374.
- [20] M. Birkholz, *Thin Film Analysis by X-ray Scattering*, Wiley-VCH Verlag GmbH Co., Weinheim, 2006.
- [21] Y. Yu, R.J. Lad, *Surf. Sci. Spectra* 4 (1998) 207–219.
- [22] C.D. Wagner, A. Joshi, *J. Electron Spectrosc. Relat. Phenom.* 47 (1988) 283–313.
- [23] C.D. Wagner, D.E. Passoja, H.F. Hillery, T.G. Kinisky, H.A. Six, W.T. Jansen, J.A. Taylor, *J. Vac. Sci. Technol.* 21 (1982) 933–944.
- [24] J.P. Chang, M.L. Green, V.M. Donnelly, R.L. Opila, J. Eng, J. Sapjeta, P.J. Silverman, B. Weir, H.C. Lu, T. Gustafsson, E. Garfunkel, *J. Appl. Phys.* 87 (2000) 4449–4455.
- [25] S.V. Okatov, A.L. Ivanovskii, *Int. J. Inorg. Mater.* 3 (2001) 923–930.
- [26] C.M. Fang, R. Metselaar, *J. Mater. Chem. Mater.* 13 (2003) 335–337.
- [27] I.J. McColm, *Ceramic Hardness*, Plenum Press, New York, 1990.
- [28] B.T. Sturtevant, M. Pereira da Cunha, R.J. Lad, *Thin Solid Films* 534 (2013) 198–204.